

Reionization during the dark ages from a cosmic axion background

Carmelo Evoli,^a Matteo Leo,^b Alessandro Mirizzi,^{c,d} Daniele Montanino^{e,f}

^aGran Sasso Science Institute, Viale Francesco Crispi 7, 67100 L'Aquila, Italy.

^bInstitute for Particle Physics Phenomenology, Department of Physics, Durham University, Durham DH1 3LE, U.K.

^cDipartimento Interateneo di Fisica “Michelangelo Merlin,” Via Amendola 173, 70126 Bari, Italy.

^dIstituto Nazionale di Fisica Nucleare - Sezione di Bari, Via Amendola 173, 70126 Bari, Italy.

^eDipartimento di Matematica e Fisica “Ennio De Giorgi,” Via Arnesano, 73100 Lecce, Italy.

^fIstituto Nazionale di Fisica Nucleare - Sezione di Lecce, Via Arnesano, 73100 Lecce, Italy.

E-mail: carmelo.evoli@gssi.infn.it, matteo.leo@durham.ac.uk,
alessandro.mirizzi@ba.infn.it, daniele.montanino@le.infn.it.

Abstract. Recently it has been pointed out that a cosmic background of relativistic axion-like particles (ALPs) would be produced by the primordial decays of heavy fields in the post-inflation epoch, contributing to the extra-radiation content in the Universe today. Primordial magnetic fields would trigger conversions of these ALPs into sub-MeV photons during the dark ages. This photon flux would produce an early reionization of the Universe, leaving a significant imprint on the total optical depth to recombination τ . Using the current measurement of τ and the limit on the extra-radiation content ΔN_{eff} by the Planck experiment we put a strong bound on the ALP-photon conversions. Namely we obtain upper limits on the product of the photon-ALP coupling constant $g_{a\gamma}$ times the magnetic field strength B down to $g_{a\gamma}B \gtrsim 6 \times 10^{-18} \text{GeV}^{-1} \text{nG}$ for ultralight ALPs.

Contents

1	Introduction	1
2	Cosmic ALP background	2
3	ALP-photon conversions in the Early Universe	5
3.1	ALP-photon conversions	5
3.2	Universe expansion	8
3.3	Photon absorption during recombination	9
3.4	Approximate expression for ALP-photon conversions	12
4	Our bound on ALPs from reionization	14
4.1	ALP-induced reionization	14
4.2	Constraints on the ALP conversions from the optical depth	14
5	Discussion and Conclusions	15

1 Introduction

Ultralight axion-like particles (ALPs) with a two-photon coupling $a\gamma\gamma$ are predicted by several extensions of the Standard Model, like four-dimensional ordinary and supersymmetric models (see e.g. [1, 2]), Kaluza-Klein theories (see e.g. [3]) and especially string theories (see e.g. [4–6]) (for a review, see [7]). The two-photon vertex allows for photon-axion mixing in external magnetic fields. This effect leading to oscillations of photons into ALPs is the basis of direct search carried on through (a) Light-Shining-Through-Wall experiments (e.g. ALPS at DESY [8]) aiming both for production and detection of ALPs in laboratory, (b) Helioscopes (e.g. CAST experiment at CERN [9] and the future IAXO project [10]) aiming at detecting solar ALPs produced by their conversions into photons inside of a strong magnet pointing towards the Sun, (c) Haloscopes (e.g. the resonant cavity ADMX experiment [11] at Livermore or the proposed dish antenna technique [12]) directly searching for galactic halo dark matter ALPs in the laboratory via their coupling to the photon. See [13] for a recent review on the experimental searches of ALPs.

The presence of cosmic magnetic fields also allows for signatures of ALPs in different astrophysical and cosmological observations. Indeed, photon-axion conversions in large-scale cosmic magnetic fields would reduce the opacity of the universe to TeV photons, explaining the anomalous spectral hardening found in the Very-High-Energy gamma-ray spectra [14–22]. Moreover, in the presence of primordial magnetic fields also the Cosmic Microwave Background (CMB) spectrum would be distorted by conversions into ALPs allowing one to put strong bounds on this mechanism [23–25]. (For a wide review on axion cosmology see [26].) Conversions of CMB photons into the magnetic fields of Galaxy Clusters have also been recently considered to get sharp constraints on the mixing [27].

An intriguing connection between ALPs and cosmology has been proposed few years ago in relation to the possible relativistic extra-radiation in the Universe, parametrized as an excess with respect to the known neutrino species $\Delta N_{\text{eff}} = N_{\text{eff}} - 3.046$ [28]. The 2015 data from the satellite experiment Planck combined with other astrophysical measurements give

$N_{\text{eff}} = 3.15 \pm 0.23$ at 68 % CL [29].¹ Therefore, even if the amount of possible extra-radiation has been significantly reduced with respect to previous indications [30], the possibility of a value of N_{eff} larger than the standard one is still a possibility. String theory models present opportunities to link the extra-radiation with ALPs [31–34]. Indeed these models often possess heavy moduli fields which need to decay after the inflation in order not to dominate the energy density of the Universe during the radiation era. In addition to the decay modes to visible sector of Standard Model (SM) particles, these fields may also decay to (effectively) massless weakly coupled particles from the hidden sector, such as ALPs and hidden photons. These ultralight particles are so weakly coupled to the SM particles that do not thermalize and contribute to the extra-radiation today [34]. In particular the cosmic ALP background produced by the moduli decay would be present today as diffuse radiation in the energy range between 100 eV to a keV. At this regard it has been proposed that the observed soft X-ray excesses in many Galaxy Clusters may be explained by the conversion of the cosmic ALP background radiation into photons in the Cluster magnetic field [35–37].

Assuming that the amount of extra-radiation compatible with the latest Planck data is composed by ALPs produced by moduli decays, this would have a strong impact on the thermal history of the Universe. Indeed the presence of a primordial magnetic field would inevitably trigger conversions between these cosmic ALPs and photons, whose impact on cosmological observables would be useful to get strong constraints on the photon-ALP coupling as discussed in [38]. In this context, we focus on ALP-photon conversions during the dark ages (at redshift $6 \lesssim z \lesssim 1100$). The produced high-energy photons [$E \lesssim \mathcal{O}(\text{MeV})$] would ionize the recently formed light atoms of Hydrogen and Helium [39]. Remarkably, even conversion probabilities at a level $\lesssim 10^{-9}$ would have a dramatic impact on the optical depth of the Universe τ . Using the latest measurement of τ by the Planck experiment [29] it would be possible to put strong constraints on this mechanism. Our work is devoted to discuss in detail this effect. In Sec. 2 we characterize the cosmic ALP background flux produced by moduli decays. In Sec. 3 we discuss the conversions of these cosmic ALPs into photons in the primordial B -fields. In Sec. 4 we show the impact of the ALP-photon conversions on the reionization and we present our bound from the cosmic optical depth. Finally in Sec. 5 we comment on our results and we conclude. It follows an Appendix where we present technical details on the derivation of the approximate expression of the ALP-photon conversion probability used in our work.

2 Cosmic ALP background

A generic feature of the four-dimensional effective theories arising from compactifications of string theory is the presence of massive scalar particles, dubbed moduli, with gravitational strength coupling. The total decay rate of moduli (into ALPs and SM particles) during the post-inflation epoch is given by [34]

$$\Gamma_{\Phi} = \frac{\kappa^2}{4\pi} \frac{m_{\Phi}^3}{M_{\text{pl}}^2}, \quad (2.1)$$

where $M_{\text{pl}} = 2.4 \times 10^{18}$ GeV is the Planck mass, m_{Φ} is the modulus mass and κ is a constant of order $\mathcal{O}(1)$. The SM particles from moduli decays would rapidly thermalize at the reheating

¹Note that the value of N_{eff} quoted by Planck would change depending on the dataset used and on the combination with other experiments.

temperature

$$T_{\text{reheat}} \sim \frac{m_{\Phi}^{3/2}}{M_{\text{pl}}^{1/2}} \sim 1 \text{ GeV} \left(\frac{m_{\Phi}}{10^6 \text{ GeV}} \right)^{3/2}. \quad (2.2)$$

Moduli can also decay into light states from the hidden sector, like ALPs, with initial energy $\varepsilon_a = m_{\Phi}/2$ and decay rate given by $\Gamma_a = B_a \Gamma_{\Phi}$ with B_a the branching ratio in ALPs. If these ALPs are weakly coupled to SM, they do not thermalize and remain till now as dark radiation, with typical energy today $\varepsilon_a \sim \mathcal{O}(100)$ eV for moduli masses $m_{\Phi} \sim 10^6$ GeV. The ALP spectrum has been calculated as in [34]. The Boltzmann equations for moduli number density n_{Φ} , and for ALPs and standard radiation ρ are respectively

$$\begin{aligned} \dot{n}_{\Phi} + 3Hn_{\Phi} &= -\Gamma_{\Phi} n_{\Phi}(t), \\ \dot{\rho} + 4H\rho &= \Gamma_{\Phi} m_{\Phi} n_{\Phi}(t). \end{aligned} \quad (2.3)$$

The Friedmann-Robertson-Walker equation

$$H(t) = \frac{\dot{R}}{R} = \sqrt{\frac{m_{\Phi} n_{\Phi}(t) + \rho(t)}{3M_{\text{pl}}^2}}, \quad (2.4)$$

closes the system, where $H(t)$ is the Hubble parameter, expressed in terms of the scale factor of the Universe $R(t)$. We assign $R(t_0) = 1$ with t_0 the age of the Universe. With the following change of variables $t = \theta \cdot \Gamma_{\Phi}^{-1}$, $n_{\Phi}(t) = \nu(\theta) \cdot N_{\Phi} \eta^3$, $\rho(t) = \sigma(\theta) \cdot N_{\Phi} m_{\Phi} \eta^3$, $R(t) = x(\theta)/\eta$, $H(t) = x'(\theta)/x(\theta) \cdot \Gamma_{\Phi}$, with N_{Φ} initial comoving number of moduli and

$$\eta = \left(\frac{3M_{\text{pl}}^2}{N_{\Phi} m_{\Phi}} \right)^{1/3} \Gamma_{\Phi}^{2/3}, \quad (2.5)$$

with initial conditions $x(0) = 0$, $\nu x^3 \rightarrow 1$ and $\sigma x^4 \rightarrow 0$ for $\theta \rightarrow 0$, the previous equations can be reduced to the following *universal* (i.e., independent from physical quantities) equation

$$h(\theta) = \frac{x'(\theta)}{x(\theta)} = \left[\frac{e^{-\theta}}{x^3(\theta)} + \frac{1}{x^4(\theta)} \int_0^{\theta} d\xi e^{-\xi} x(\xi) \right]^{1/2}. \quad (2.6)$$

This equation can be integrated numerically. For small θ the evolution is matter dominated ($x \sim \theta^{2/3}$) while for large θ the evolution is radiation dominated ($x \sim \theta^{1/2}$).

The number density of ALPs per unit of energy and comoving volume $\mathcal{N}_a(E, t)$ follows the Boltzmann equation

$$\left[\frac{\partial}{\partial t} - H(t)E \frac{\partial}{\partial E} - H(t) \right] \mathcal{N}_a = 2B_a \Gamma_{\Phi} \delta \left(E - \frac{m_{\Phi}}{2} \right) N_{\Phi} e^{-\Gamma_{\Phi} t}, \quad (2.7)$$

where we suppose that the moduli decay at rest (since $T_{\text{reheat}} \ll m_{\Phi}$) and the factor 2 on the right side accounts for the fact that two ALPs are produced for each moduli decay. Using the comoving energy $E_0 = ER(t) = Ex/\eta$ and x as independent variables we can rewrite the previous equation as

$$\left(x \frac{\partial}{\partial x} - 1 \right) \mathcal{N}_a = \frac{2B_a}{h(\theta(x)) \eta E_0} \delta \left(x - \eta \frac{2E_0}{m_{\Phi}} \right) N_{\Phi} e^{-\theta(x)}. \quad (2.8)$$

This equation can be integrated from $x = 0$ to $x > 2\eta E_0/m_\Phi$ giving

$$\frac{dn_a(E, z)}{dE} = (1+z)^3 \mathcal{N}_a(E, t) = \frac{2N_\Phi B_a}{\varepsilon_a} (1+z)^2 \varphi\left(\frac{E}{(1+z)\varepsilon_a}\right), \quad (2.9)$$

where

$$\varphi(x) = -\frac{d}{dx} e^{-\theta(x)}, \quad (2.10)$$

and $\varepsilon_a = m_\Phi/2\eta$ and we have used $x/\eta = R(t) = (1+z)^{-1}$ and $h = (x\theta'(x))^{-1}$. The factor $n_a = 2N_\Phi B_a$ is the total density of ALPs today. The function $\varphi(x)$ can be calculated numerically from Eq. (2.6). A handy and very accurate approximation is a quasi-thermal spectrum given by

$$\varphi(x) \simeq \frac{\alpha K^{\alpha/\beta}}{\Gamma\left(\frac{\alpha}{\beta}\right)} x^\alpha \exp(-Kx^\beta), \quad (2.11)$$

where Γ is the Euler gamma function, $\alpha = 1.434$, $\beta = 1.980$ and $K = 0.445$.

Since N_Φ and B_a are unknown, it is convenient to write Eq. (2.9) in terms of observable parameters. The density of SM radiation after moduli decay can be written as

$$\rho_{\text{SM}}(t_D) = \eta^{-1} J \cdot m_\Phi N_\Phi (1 - B_a) \cdot \frac{1}{R^4(t_D)}, \quad (2.12)$$

where $t_D \sim \mathcal{O}(10\Gamma_\Phi^{-1})$ and $J = \int_0^\infty d\theta e^{-\theta} x(\theta) \simeq 1.078$. This radiation can be observed nowadays as CMB radiation. Using $\rho \propto (g^*)^{-1/3} R^{-4}$ we have

$$\rho_{\text{CMB}} = \left(\frac{11}{4}\right)^{1/3} \cdot \left(\frac{22}{43}\right) \cdot \left[\frac{g^*(T_D)}{g^*(T_\nu)}\right]^{1/3} \cdot R^4(t_D) \cdot \rho_{\text{SM}}(t_D), \quad (2.13)$$

where $\rho_{\text{CMB}} = 2 \times 10^{-51} \text{ GeV}^4$ is the present CMB energy density, $g^*(T_\nu) = 10.25$ the number of degree of freedom at the neutrino decoupling, $g^*(T_D)$ the number of degree of freedom at the end of moduli decay, the factor $(11/4)^{1/3}$ accounts for the photon reheating due to e^+e^- annihilation, while $22/43$ is the fraction of radiation in visible form after neutrino decoupling.

Note that in principle is not easy to determine $g^*(T_D)$ because $T_D \lesssim T_{\text{reheat}}$ is not a well defined quantity. However, is reasonable to expect that moduli decay occurs well before QCD phase transition [Eq. (2.2)], where $g^*(T_{\text{QCD}}) = 61.75$. For $T_D > T_{\text{QCD}}$, $g^*(T)$ is a smooth function of temperature. We will see that the final ALPs density and energy depends mildly from $g^*(T_D)$ (as $[g^*(T_D)]^{1/12}$). Moreover, $g^*(T_D)$ can be reabsorbed by a redefinition the (unknown) moduli mass. For this reason the exact determination of $g^*(T_D)$ is not crucial.

We also remind that B_a will depend to the final observable extra-radiation ΔN_{eff} by the relation [34]:

$$\Delta N_{\text{eff}} = \frac{43}{7} \frac{B_a}{1 - B_a} \left[\frac{g^*(T_\nu)}{g^*(T_D)}\right]^{1/3}, \quad (2.14)$$

so that

$$B_a \simeq 0.29 \left(\frac{g_D^*}{61.75}\right)^{1/3} \Delta N_{\text{eff}}. \quad (2.15)$$

Eq. (2.13) can be inverted to obtain N_Φ . After straightforward calculations we can infer the total density of ALPs at $t = t_0$

$$n_a = 2N_\Phi B_a = 133 \text{ m}^{-3} \left(\frac{\tilde{m}_\Phi}{\text{PeV}}\right)^{1/2} \Delta N_{\text{eff}}, \quad (2.16)$$

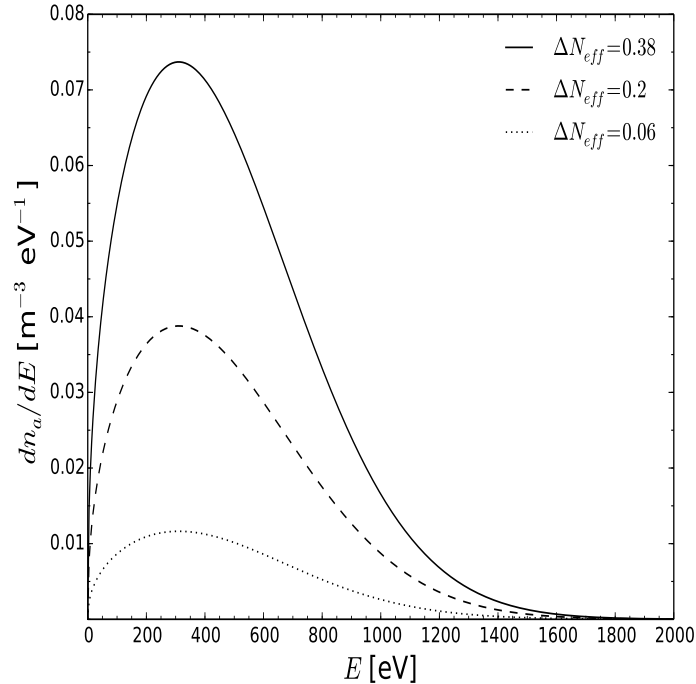


Figure 1. Cosmic ALP spectrum today for different values of ΔN_{eff} . (see the text for details)

where we have defined the “effective” moduli mass

$$\tilde{m}_\Phi = (1 - B_a)^{1/2} \kappa^2 \left(\frac{g_D^*}{61.75} \right)^{1/6} m_\Phi . \quad (2.17)$$

The actual ($z = 0$) ALP spectrum thus can be written as

$$\frac{dn_a(E)}{dE} = \frac{n_a}{\varepsilon_a} \varphi \left(\frac{E}{\varepsilon_a} \right) , \quad (2.18)$$

with

$$\varepsilon_a = 412 \left(\frac{\tilde{m}_\Phi}{\text{PeV}} \right)^{-1/2} \text{eV} . \quad (2.19)$$

The ALP spectrum in Eq. (2.18) is represented in Fig. 1 for the benchmark parameters in parenthesis of Eq. (2.15)–(2.17). For the amount of ALP extra-radiation we assume $\Delta N_{\text{eff}} = 0.38$ (continuous curve) corresponding to the 1σ range of Planck 2015 analysis [29], $\Delta N_{\text{eff}} = 0.2$ (dashed curve) and $\Delta N_{\text{eff}} = 0.06$ (dotted curve) corresponding to the 2σ sensitivity of the future EUCLID mission [40].

3 ALP-photon conversions in the Early Universe

3.1 ALP-photon conversions

Photon-ALP mixing occurs in the presence of an external magnetic field \mathbf{B} due to the Lagrangian [41–43]

$$\mathcal{L}_{a\gamma} = -\frac{1}{4} g_{a\gamma} F_{\mu\nu} \tilde{F}^{\mu\nu} a = g_{a\gamma} \mathbf{E} \cdot \mathbf{B} a , \quad (3.1)$$

where $g_{a\gamma}$ is the photon-ALP coupling constant (which has the dimension of an inverse energy).

We assume a beam of energy E propagating along the x_3 direction in a cold ionized and magnetized medium. At first we restrict our attention to the case in which the magnetic field \mathbf{B} is homogeneous. We denote by \mathbf{B}_T the transverse magnetic field, namely its component in the plane normal to the beam direction and we choose the x_2 -axis along \mathbf{B}_T so that B_1 vanishes. The linear photon polarization state parallel to the transverse field direction \mathbf{B}_T is then denoted by A_{\parallel} and the orthogonal one by A_{\perp} . Neglecting for the moment incoherent scattering, the linearized equations of motion for the ALP state a and for the two polarization states of the photons are [41]

$$\left(E - i\frac{\partial}{\partial x_3} + \mathcal{M}\right) \begin{pmatrix} A_{\perp} \\ A_{\parallel} \\ a \end{pmatrix} = 0, \quad (3.2)$$

where the mixing matrix can be written as [23, 24]

$$\mathcal{M}_0 = \begin{pmatrix} \Delta_{\perp} & 0 & 0 \\ 0 & \Delta_{\parallel} & \Delta_{a\gamma} \\ 0 & \Delta_{a\gamma} & \Delta_a \end{pmatrix}, \quad (3.3)$$

whose elements are [41] $\Delta_{\perp} \equiv \Delta_{\text{pl}} + \Delta_{\perp}^{\text{CM}}$, $\Delta_{\parallel} \equiv \Delta_{\text{pl}} + \Delta_{\parallel}^{\text{CM}} + \Delta_{\text{CMB}}$, $\Delta_{a\gamma} \equiv g_{a\gamma} B_T/2$ and $\Delta_a \equiv -m_a^2/2E$, where m_a is the ALP mass. The term $\Delta_{\text{pl}} \equiv -\omega_{\text{pl}}^2/2E$ accounts for plasma effects, where ω_{pl} is the plasma frequency expressed as a function of the electron density in the medium n_e as $\omega_{\text{pl}} \simeq 3.69 \times 10^{-11} \sqrt{n_e/\text{cm}^{-3}} \text{ eV}$. The terms $\Delta_{\parallel,\perp}^{\text{CM}}$ describe the Cotton-Mouton effect, i.e. the birefringence of fluids in the presence of a transverse magnetic field. A vacuum Cotton-Mouton effect is expected from QED one-loop corrections to the photon polarization in the presence of an external magnetic field $\Delta_{\text{QED}} = |\Delta_{\perp}^{\text{CM}} - \Delta_{\parallel}^{\text{CM}}| \propto B_T^2$, but this effect is completely negligible in the present context, as we will show in Sec. 3.4. Recently it has been realized that also background photons can contribute to the photon polarization. At this regard a guaranteed contribution is provided by the CMB radiation, leading to $\Delta_{\text{CMB}} \propto \rho_{\text{CMB}}$ [44]. We will show in Sec. 3.4 how this term would play a crucial role for the development of the conversions at large redshift during the recombination epoch. An off-diagonal Δ_R would induce the Faraday rotation, which is however totally irrelevant at the energies of our interest, and so it has been dropped. For the relevant parameters, we numerically find

$$\begin{aligned} \Delta_{a\gamma} &\simeq 1.52 \times 10^{-8} \left(\frac{g_{a\gamma}}{10^{-17} \text{ GeV}^{-1}}\right) \left(\frac{B_T}{10^{-9} \text{ G}}\right) \text{ Mpc}^{-1}, \\ \Delta_a &\simeq -7.8 \times 10^5 \left(\frac{m_a}{10^{-10} \text{ eV}}\right)^2 \left(\frac{E}{\text{keV}}\right)^{-1} \text{ Mpc}^{-1}, \\ \Delta_{\text{pl}} &\simeq -1.1 \times 10^{-2} \left(\frac{E}{\text{keV}}\right)^{-1} \left(\frac{n_e}{10^{-7} \text{ cm}^{-3}}\right) \text{ Mpc}^{-1}, \\ \Delta_{\text{QED}} &\simeq 4.1 \times 10^{-18} \left(\frac{E}{\text{keV}}\right) \left(\frac{B_T}{10^{-9} \text{ G}}\right)^2 \text{ Mpc}^{-1}, \\ \Delta_{\text{CMB}} &\simeq 0.80 \times 10^{-10} \left(\frac{E}{\text{keV}}\right) \text{ Mpc}^{-1}. \end{aligned} \quad (3.4)$$

For the above estimates that we will use in the following as benchmark values, we refer to the following physical inputs: The strength of B -fields and the electron density n_e in the previous equations are typical values for the intergalactic medium. Moreover, we note that in the equations enter only the product $g_{a\gamma}B_T$. Since we will be interested in possible ALP-photon conversions during the recombination epoch in the Early Universe, we require $g_{a\gamma}B_T \lesssim 10^{-13}$ GeV nG for $m_a \lesssim 10^{-9}$ eV in order to avoid an excessive distortion of the CMB spectrum [25] caused by the conversions during that phase. This requirement satisfies also the direct experimental bound on $g_{a\gamma}$ obtained by the CAST experiment [9], the globular-cluster limit [45] and the one for ultra-light ALPs from the absence of γ -rays from SN 1987A [46]. Concerning the ALP energy today the bulk of the spectrum is in the range $E \in [100, 800]$ eV (see Fig. 1). Finally, we will assume $m_a \ll \omega_{\text{pl}}$, neglecting the term Δ_a in the evolution, since a value of m_a much larger than ω_{pl} would suppress the conversions.

We note that in the case of a homogeneous magnetic field, the ALP-photon mixing described by Eq. (3.2) reduces to a 2×2 problem involving only the (A_{\parallel}, a) . Since in the following we will consider cosmic ALP inter-converting into photons in the primordial magnetic fields, we have to deal with a more general situation than the one of the homogeneous case considered above. The possible existence of a primordial magnetic field of cosmological origin has been the subject of an intense investigation during the last few decades [47]. However despite these efforts, there is no astrophysical evidence for primordial magnetic fields, and only upper limits are reported. In particular primordial B -fields would have an impact on CMB anisotropies. Overall, Planck data constrain the amplitude of primordial B -fields to be less than a few nG coherent on a scale $l \sim \mathcal{O}(1 \text{ Mpc})$ [48]. Therefore, the primordial B -field has a domain-like structure with size set by its coherence length. The strength of \mathbf{B} is assumed to be the same in every domain, but its direction changes in a random way from one cell to another. Because of this, A_{\parallel} in one region or cell is not the same as A_{\parallel} in the next one. Therefore the propagation over many magnetic domains represents a full 3-dimensional case. In order to treat this problem we consider the x_1, x_2, x_3 coordinate system and expand the photon polarization states on this basis of coordinates, i.e. (A_1, A_2) .

We take the coordinate basis as fixed once and for all, and – labelling with ψ_p the angle between B_T and the x_2 axis in the generic p -th domain ($1 \leq p \leq n$) – we treat every ψ_p as a random variable in the range $0 \leq \psi_p < 2\pi$. During their propagation with a total path L , the beam crosses $n = L/l$ domains, where l is the size of each domain. Then the set $\{(B_T)_p\}_{1 \leq p \leq n}$ represents a given random realization of the beam propagation corresponding to the the angles $\{\psi_p\}_{1 \leq p \leq n}$. Since we are interested only in the average of the conversion probability, we do not need to make any assumption on the probability distribution function of the $(B_T)_p$'s. In the following for simplicity we denote with B and B_T the r.m.s. of the magnetic field and of its transversal component on all possible configurations respectively ($B \equiv \sqrt{\langle B^2 \rangle}$). For symmetry reasons of course we have $B_T^2 = 2B^2/3$. We remark that this model with constant magnetic field in each cell is unrealistic because the condition $\nabla \cdot \mathbf{B} = 0$ cannot be satisfied on the boundary of cells, however is a good approximation for practical purposes. In the Appendix we will show briefly how to relax this approximation.

Accordingly, in each domain the matrix \mathcal{M} takes the form [23]

$$\mathcal{M}_p = \begin{pmatrix} \Delta_{xx} & \Delta_{xy} & \Delta_{a\gamma} \sin \psi_p \\ \Delta_{yx} & \Delta_{yy} & \Delta_{a\gamma} \cos \psi_p \\ \Delta_{a\gamma} \sin \psi_p & \Delta_{a\gamma} \cos \psi_p & \Delta_a \end{pmatrix}, \quad (3.5)$$

with

$$\Delta_{xx} = \Delta_{\parallel} \sin^2 \psi_p + \Delta_{\perp} \cos^2 \psi_p , \quad (3.6)$$

$$\Delta_{xy} = \Delta_{yx} = (\Delta_{\parallel} - \Delta_{\perp}) \sin \psi_p \cos \psi_p , \quad (3.7)$$

$$\Delta_{yy} = \Delta_{\parallel} \cos^2 \psi_p + \Delta_{\perp} \sin^2 \psi_p . \quad (3.8)$$

In general the solution of this problem can be obtained in terms of the product of transfer functions for the ALP-photon ensemble across the different magnetic domains [49]. However in the case we are dealing with, since we expect small conversion probabilities, we will show in the Appendix that it is possible to adopt a perturbative approach for this calculation.

3.2 Universe expansion

The evolution of the ALP-photon beam in the homogeneous and isotropic Universe can be characterized considering the time $t \simeq x_3$ as evolution variable. Furthermore, one has to take into account the expansion of the Universe [50]. This can be accounted expressing the evolution in terms of the redshift by means of

$$\frac{dt}{dz} = - \frac{1}{(1+z)H_0 \sqrt{\Omega_{\Lambda} + \Omega_{\text{m}}(1+z)^3}} , \quad (3.9)$$

where according to the latest Planck data, the Hubble constant parameter $H_0 = (67.8 \pm 0.9)$ km s⁻¹ Mpc⁻¹, the matter density parameter $\Omega_{\text{m}} = 0.308 \pm 0.012$ and the dark energy density $\Omega_{\Lambda} = 0.6911 \pm 0.0062$ [29].

The redshift effect leaves unaltered the equations of motion [Eq. (3.2)], after an appropriate rescaling of the different parameters. Since the number density of the electrons traces that of matter, and the average number density of electrons goes as the third power of the size of the Universe, we obtain the relationship

$$n_e(z) = n_{e,0}(1+z)^3 . \quad (3.10)$$

Note that the thermal history of the electron density can be rather complicated due to the presence of reionization (at $z \lesssim 30$) and recombination into H and He (at $z \lesssim 1100$) [25]. However, since in our study we will consider ALP energies much larger than the binding energies of these light atoms, we will always consider the contribution of n_e to the plasma density ω_{pl} as if the electrons were all free, with a density obtained simply redshifting their actual one.

For the magnetic field, being frozen into the medium we have the relation

$$B(z) = (1+z)^2 B_0 , \quad (3.11)$$

where the size of each cell scales as

$$l(z) = \frac{l_0}{(1+z)} , \quad (3.12)$$

while the energy of the beam scales as

$$E(z) = E_0(1+z) , \quad (3.13)$$

where with subscript 0 we indicate the today values of the different quantities. Considering this redshift relation we find that the quantities in Eq. (3.4) evolve as

$$\begin{aligned}
\Delta_{a\gamma} &= \Delta_{a\gamma}^0 (1+z)^2, \\
\Delta_a &= \frac{\Delta_a^0}{(1+z)}, \\
\Delta_{\text{pl}} &= \Delta_{\text{pl}}^0 (1+z)^2, \\
\Delta_{\text{QED}} &= \Delta_{\text{QED}}^0 (1+z)^5, \\
\Delta_{\text{CMB}} &= \Delta_{\text{CMB}}^0 (1+z)^5,
\end{aligned}
\tag{3.14}$$

where the superscript 0 indicates the today value. In Fig. 2 we show the evolution of the different quantities of Eq. (3.14) [multiplied by $l(z)$] in function of the redshift z at different representative energies of the ALP spectrum for $g_{a\gamma} B = 10^{-17} \text{GeV}^{-1} \text{nG}$. From the scaling law one realizes that for $z \gg 10^3$, Δ_{CMB} exceeds all the other quantities. In particular, being larger than the off-diagonal quantity $\Delta_{a\gamma}$, it suppresses the ALP oscillations. Therefore, in the following we will start the characterization of the conversions at $z \lesssim 1800$. [Note that CMB effect was not included in [38], where effects of conversions at earlier epochs (e.g. during Big Bang Nucleosynthesis) was discussed.] In this range the Δ_{QED} term is completely negligible. As the Universe expands eventually there is a point where $|\Delta_{\text{CMB}} + \Delta_{\text{pl}}|$ cancels (continuous black curve). When this occurs the diagonal term in the Hamiltonian [Eq. (3.4)] vanishes. This implies that one can have large *resonant* conversion effects there. At lower redshift one expects the ALP conversions to be suppressed again due the dominance of the plasma term Δ_{pl} over $\Delta_{a\gamma}$. Therefore, we expect only a narrow range in z where ALP-photon conversions would occur.

We mention that in the presence of a finite ALP mass ($m_a \lesssim 10^{-10} \text{ eV}$) it would be possible to encounter also a $\omega_{\text{pl}} = m_a$ resonance that would leave a further imprint on the pattern of conversions. Conversely, for an ALP mass greater than 10^{-10} eV no resonance is allowed and then $\gamma \leftrightarrow a$ oscillations would be suppressed.

3.3 Photon absorption during recombination

As discussed before, ALP conversions into photons start at $z \sim 10^3$, i.e. in the phase of matter-radiation decoupling started at $z \sim 1100$. At this epoch, at $T \sim 0.3 \text{ eV}$, the process $H + \gamma \leftrightarrow p + e^-$ goes out of equilibrium, leading the the *recombination* of electrons and protons into Hydrogen and Helium. Following this event, in the so-called *dark ages*, most of the intergalactic matter was composed largely of neutral Hydrogen and Helium, being the fraction of ionized Hydrogen (normalized to 1 for full ionization) $X_{\text{H}} \sim 10^{-4}$. This epoch lasted from $z \sim 1100$ to $z \sim 30$. The emergence of the first luminous sources at $z \sim 30$ corresponds to the period during which the gas in the Universe went from being almost completely neutral to a state in which it became almost completely ionized. In fact, the *reionization* of the Universe was complete at about redshift $z \sim 6$ [51]. The reionization sources may have been stars, galaxies, quasars, or some combination of the above [52]. A large amount of experimental efforts, as the LOFAR telescope [53], aims at measuring the neutral gas fraction in the Universe as a function of redshift in order to have a more detailed understanding of the astrophysical processes at these earlier epochs.

In Fig. 3 we show as a continuous curve the evolution of X_{H} after recombination in the standard scenario (as computed with the RECFAST code [54]), and assuming that reionization has occurred instantaneously at $z = 6$. Photons produced by ALP conversions during

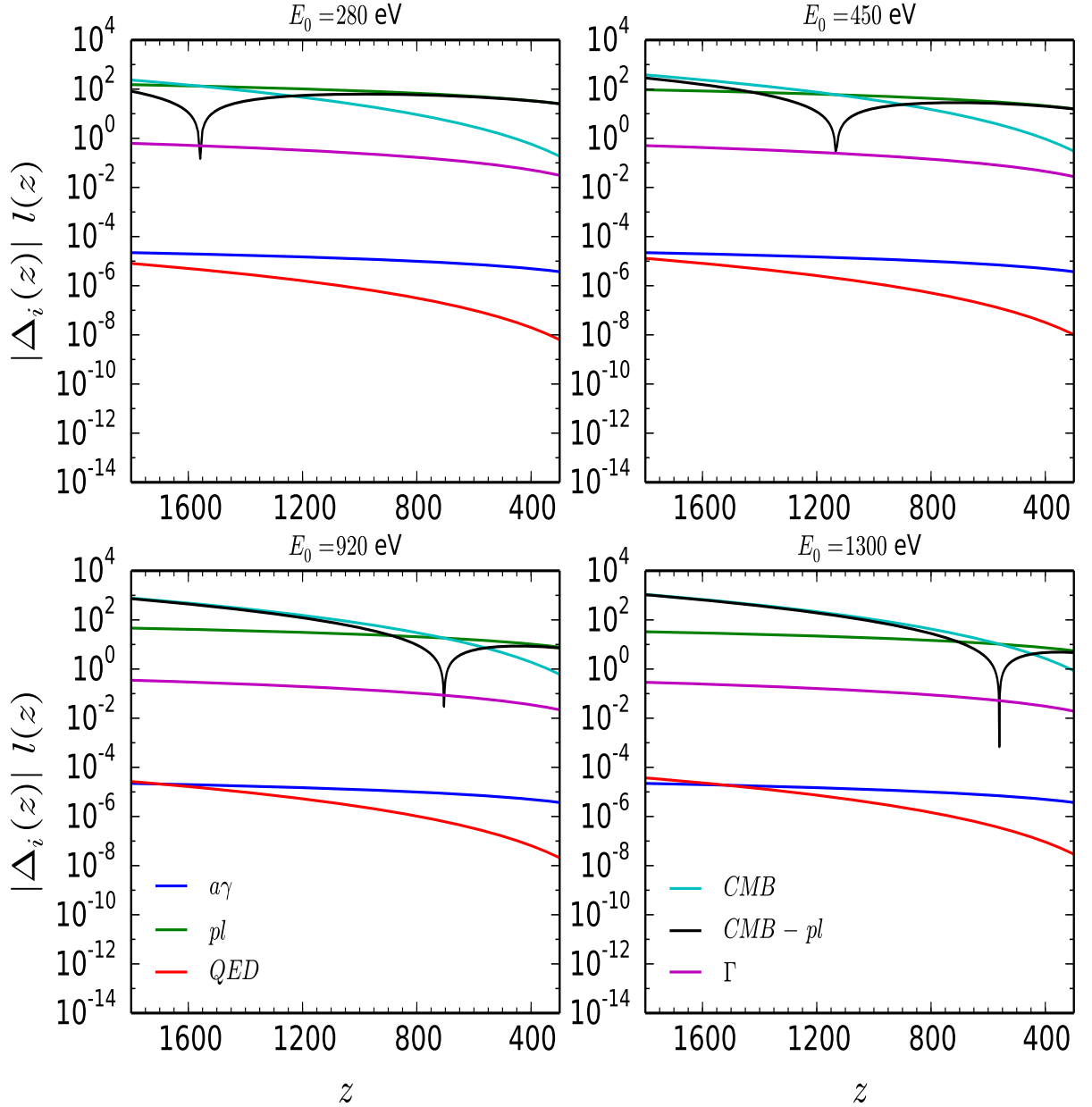


Figure 2. Evolution with redshift of the different quantities $\Delta_{a\gamma}$, Δ_{pl} , Δ_{QED} , $|\Delta_{CMB} + \Delta_{pl}|$ and Γ multiplied for $l(z)$.

the dark ages have an energy $E \in [0.1, 0.8]$ MeV. Therefore, they are much more energetic than the CMB photons and would ionize the recently formed neutral atoms much earlier than the standard reionization.

The photon absorption on electrons and atoms adds a damping term in the ALP-photon

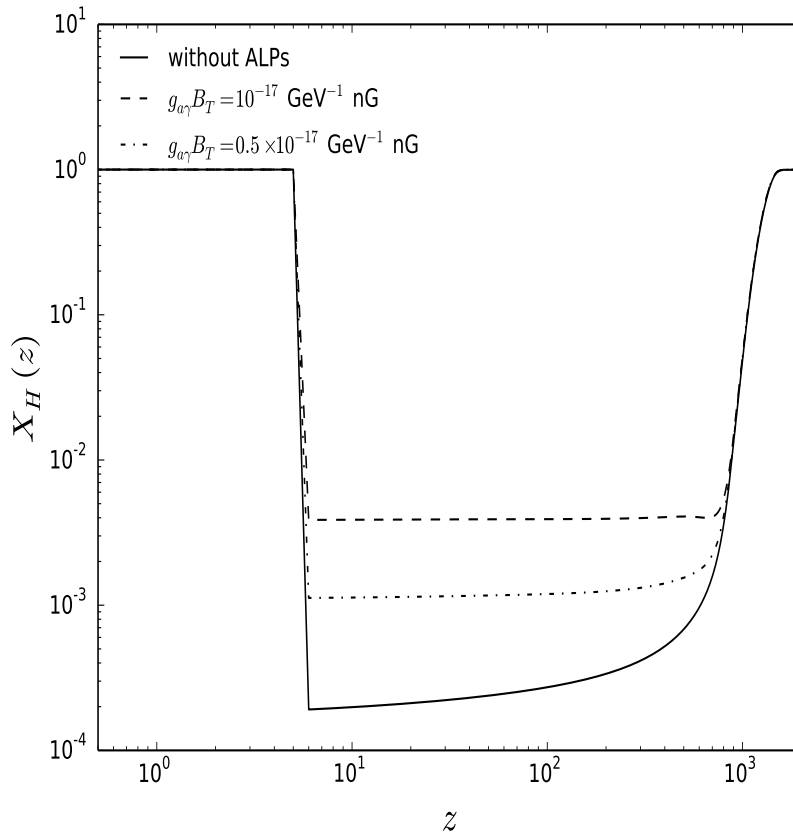


Figure 3. Fraction of ionized hydrogen X_H (normalized to 1 for full ionization) in function of redshift z without (continuous curve) and with ALP conversions for $g_{a\gamma} B = 10^{-17} \text{GeV}^{-1} \text{nG}$ (dashed curve) and $g_{a\gamma} B = 5 \times 10^{-18} \text{GeV}^{-1} \text{nG}$ (dot-dashed curve). We assume $\Delta N_{\text{eff}} = 0.38$.

Hamiltonian [17]

$$\mathcal{M} \rightarrow \mathcal{M} + \text{diag}\left(-i\frac{\Gamma}{2}, -i\frac{\Gamma}{2}, 0\right) . \quad (3.15)$$

In the absorption term one has to take into account the photo-electric and to the Compton effect. The absorption term assumes then the form

$$\Gamma = \sigma_{\text{KN}} n_e + \sigma_{\text{H}}^{\text{PE}} n_{\text{H}} + \sigma_{\text{He}}^{\text{PE}} n_{\text{He}} , \quad (3.16)$$

where σ_{KN} refers to the Klein-Nishina cross-sections for the Compton effect on (free or bound) electrons, while $\sigma_{\text{H}}^{\text{PE}}, \sigma_{\text{He}}^{\text{PE}}$ refer to the photo-electric effect on H and He, respectively. These latter cross sections are taken from [55].² Moreover we take

$$n_e = \left(1 - \frac{Y_{\text{He}}}{2}\right) n_B , \quad (3.17)$$

$$n_{\text{H}} = (1 - Y_{\text{He}}) n_B , \quad (3.18)$$

$$n_{\text{He}} = \frac{Y_{\text{He}}}{4} n_B . \quad (3.19)$$

²Fortran subroutines for the calculation of photo-electric cross sections can be found at the following URL: <http://www.pa.uky.edu/~verner/photo.html>

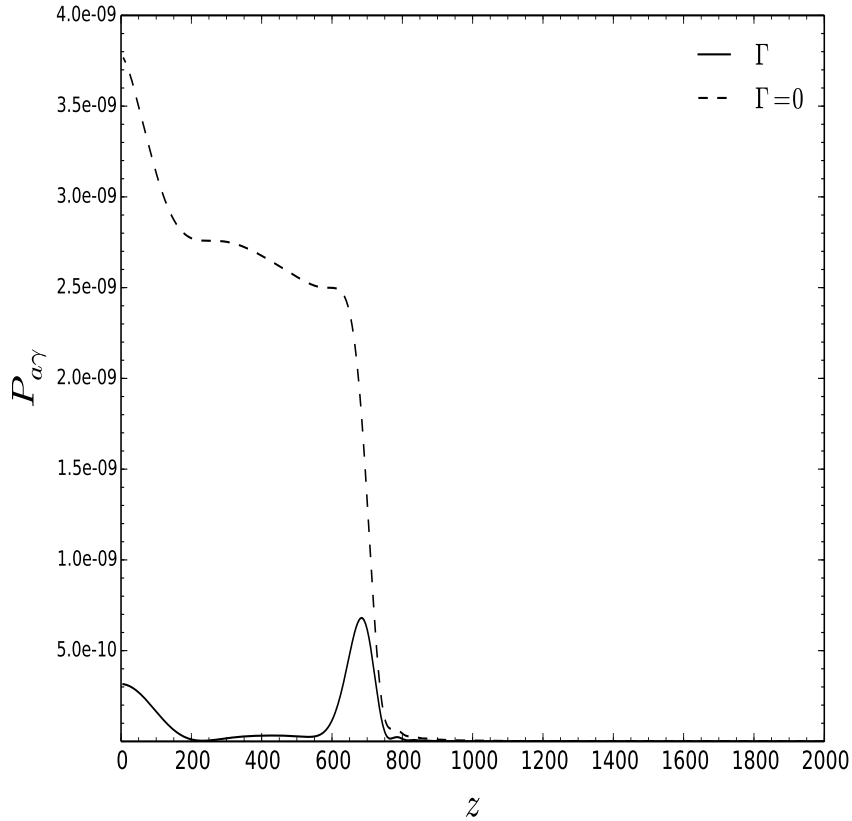


Figure 4. Conversion probability $P_{a\gamma}$ in function of the redshift z for ALP energy $E_0 = 920$ eV for $g_{a\gamma}B = 10^{-17}\text{GeV}^{-1}\text{nG}$ with absorption Γ (continuous curve) and with $\Gamma = 0$ (dashed curve).

where $Y_{\text{He}} = 0.2465$ is the Helium fraction and $n_B = 2.482 \times 10^{-7} \text{ cm}^{-3}$ is the baryon density [56]. The quantity $\Gamma l(z)$ in function of the redshift has been plotted in Fig. 2.

3.4 Approximate expression for ALP-photon conversions

We finally note that from Fig. 2 it results that

$$\Delta_{a\gamma} \ll \Delta_{\text{pl}} , \quad (3.20)$$

independently on the redshift. This would allow us to find perturbatively a solution of the evolution equation [Eq. (3.2)] (see Appendix). We find a recursive expression for the average conversion probability in the n -th magnetic domain

$$P_{a\gamma}^{(n+1)} = \left[P_{a\gamma}^{(n)} + (\Delta_{a\gamma}^{(n)} l_n)^2 \text{sinc}^2 \frac{k_n l_n}{2} \right] e^{-\Gamma_n l_n} \quad (3.21)$$

where the subscript n refer to the values of the different quantities at redshift z_n . In the previous equation

$$k = \Delta_{\text{CMB}} + \Delta_{\text{pl}} , \quad (3.22)$$

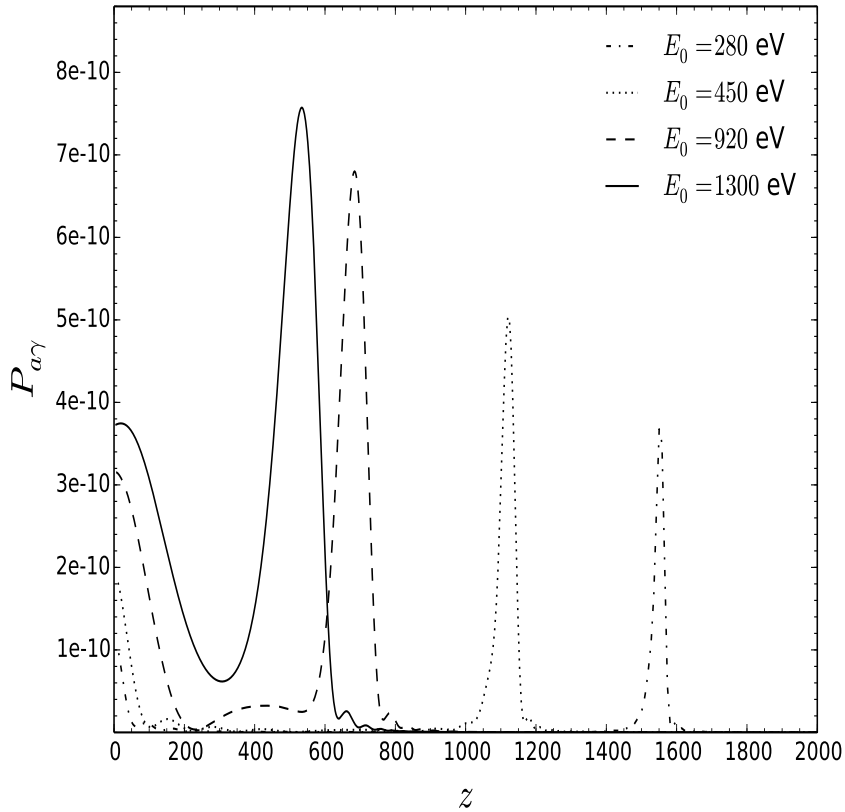


Figure 5. Conversion probability $P_{a\gamma}$ in function of the redshift z for different representative energies of the ALP spectrum for $g_{a\gamma}B = 10^{-17}\text{GeV}^{-1}\text{nG}$.

(we remark that $\Delta_{\text{pl}} < 0$) and the function

$$\text{sinc } x = \frac{\sin x}{x} . \quad (3.23)$$

In Fig. 4 we show the conversion probability $P_{a\gamma}$, obtained from Eq. (3.21), in function of the redshift z for a representative ALP energy $E_0 = 920$ eV for $g_{a\gamma}B = 10^{-17}\text{GeV}^{-1}\text{nG}$ with absorption Γ (continuous curve) and with $\Gamma = 0$ (dashed curve). In the case with $\Gamma = 0$ we realize that the conversions in photons occur resonantly at $z \simeq 800$ when $k = 0$ (see Fig. 2) and then would smoothly grow at a lower z . Instead, in the presence of absorption the conversions are heavily suppressed just after the resonance point.

In Fig. 5 we show the conversion probability $P_{a\gamma}$ for $g_{a\gamma}B = 10^{-17}\text{GeV}^{-1}\text{nG}$ obtained from Eq. (3.21) for the same energies considered in Fig. 2. We realize that the probability has a typical resonant behavior, being peaked at redshift for which $k = 0$ shown in Fig. 2. We also note that for the values of the different parameters $P_{a\gamma} \lesssim 10^{-9}$.

4 Our bound on ALPs from reionization

4.1 ALP-induced reionization

The photon spectrum produced by ALP conversions in the n -th cell at redshift $z = z_n$ can be written as

$$\frac{dn_\gamma}{dE(z)} = \frac{dn_a}{dE(z)} \cdot P_{a\gamma}^{(n)} , \quad (4.1)$$

where the values of the different quantities characterizing the ALP spectrum are reported in Sec. 2. Of these photons the fraction that interacts in the n -th cell is $f_S(z) = 1 - \exp(-\Gamma_n l_n)$. Each of these scattered photons together with the photo-electrons gives rise to an electromagnetic shower that would ionize the light atoms. Assuming for simplicity that only H atoms are ionized, one gets that the fraction of free electrons produced in the n -th cell

$$\Delta n_e^{\text{free}}(z) = \int dE(z) \frac{dn_\gamma}{dE(z)} \times f_S(z) \times f_I(z) \times \frac{E(z)}{13.6 \text{ eV}} , \quad (4.2)$$

where numerically [57]

$$f_I(z) = a \times \left[1 - (X_H(z))^b \right]^c , \quad (4.3)$$

with $a = 0.3846$, $b = 0.5420$ and $c = 1.1952$. The fraction of ionized H at redshift $z = z_n$ can be expressed as

$$X_H(z) = X_H^0(z) + \frac{\Delta n_e^{\text{free}}(z)}{n_H} , \quad (4.4)$$

where $X_H^0(z)$ is the value without extra-ionization. Note that in principle free electron would recombine with ionized H atoms. However, we estimated that for the values of the parameters chosen this effect is always negligible.

In Fig. 3 we compare X_H for the standard case (continuous curve) and in presence of a primordial ALP flux converting into photons with a coupling of $g_{a\gamma} B = 10^{-17} \text{ GeV}^{-1} \text{ nG}$ (dashed curve) and $g_{a\gamma} B = 5 \times 10^{-18} \text{ GeV}^{-1} \text{ nG}$ (dot-dashed curve). We assume that ALPs give $\Delta N_{\text{eff}} = 0.38$. In the presence of ALPs conversions the drop in X_H during the recombination epoch is milder leading to a difference of one order of magnitude for the case of the strongest coupling considered.

4.2 Constraints on the ALP conversions from the optical depth

In order to assess the maximum allowed contribution from cosmic ALPs to reionization we compare the total optical depth in our scenario with the value measured by the Planck collaboration. The total optical depth encountered by the photons as they travel to us from the surface of last scattering is given by:

$$\tau = \int_0^\infty n_e^{\text{free}}(z) \sigma_T \left| \frac{dt}{dz} \right| dz , \quad (4.5)$$

where $n_e^{\text{free}}(z) = X_H(z) \cdot n_H$ is the fraction of unbound electrons and σ_T is the Thomson cross section. It is then clear that this observable is sensitive to the number of extra ionizations of neutral Hydrogen or Helium atoms at $z \lesssim 1000$ induced by ALP-photon conversions.

Observational evidences (in particular from the spectra of quasars located at redshift $z \sim 6$ [51]) allows to infer that intergalactic H and He gases are fully ionized below redshift 6,

and He is also doubly ionized below redshift $z = 3$ [58]. The resulting free electron population from us to redshift $z = 6$ contributes to the total optical depth with about $\tau_{z<6} = 0.038$ [59].

Planck observations of temperature and polarization anisotropies data provided us with a measurement of the reionization optical depth [29]

$$\tau_{\text{obs}} = 0.066 \pm 0.016 , \quad (4.6)$$

at 68 % CL. Astrophysical sources (as PopIII stars or Quasars) at $z > 6$ can possibly provide enough ionizing photons (either UV or X-rays) to complete the reionization and explain the observed value. However, the effective contribution of the different kinds of reionization sources and their evolution with redshift is highly uncertain [52, 60]. As in [59] we bound the ALP contribution by imposing that:

$$\tau_{\text{ALP}} < \tau_{\text{obs}}^{2\sigma} - \tau_{z<6} \sim 0.044 , \quad (4.7)$$

where τ_{ALP} is the optical depth integrated for $z > 6$ in the presence of ALP-photon conversions and $\tau_{\text{obs}}^{2\sigma}$ is the maximum value for τ allowed (within 2σ) by Planck measurements. Notice that, in doing so, we assume that ALPs are the only source of reionization earlier than $z = 6$. This is unrealistic, since we observe galaxies at redshift higher than 6. However it provides a conservative bound. Including the contribution of other reionization sources would lead us to stronger constraints.

In Fig. 6 we show the optical depth τ as a function of $g_{a\gamma}B$ for $\Delta N_{\text{eff}} = 0.38$ (continuous curve) in agreement with the 1σ range from Planck 2015 analysis [29], $\Delta N_{\text{eff}} = 0.2$ (dashed curve) and $\Delta N_{\text{eff}} = 0.06$ (dotted curve) which corresponds to the 2σ forecast of the future EUCLID experiment [40]. Horizontally we show the 2σ band of τ from Eq. (4.6). We realize that for $\Delta N_{\text{eff}} = 0.38$ values of $g_{a\gamma}B \gtrsim 6 \times 10^{-18} \text{ GeV}^{-1} \text{ nG}$ would be excluded. The bound is worsened if less amount of extra-radiation is composed by ALPs going down to $g_{a\gamma}B \gtrsim 1.5 \times 10^{-17} \text{ GeV}^{-1} \text{ nG}$ for $\Delta N_{\text{eff}} = 0.06$. Therefore, also in the presence of a subleading content of ALP extra-radiation the bound remains impressive.

5 Discussion and Conclusions

String theory would provide an intriguing connection between the possible extra-radiation ΔN_{eff} and a flux of ultralight ALPs generated by heavy moduli decays in the post-inflation epoch. The presence of this cosmic background would have an interesting phenomenology. Indeed X-ray excesses in many Galaxy Clusters may be explained by the conversions of the this cosmic ALP background radiation into photons in the Cluster magnetic field. In the current work we have explored another possible feature of this model. Indeed, the presence of primordial magnetic fields in the Early Universe would trigger ALP-photon conversions during the dark ages, producing a flux of sub-MeV photons that would ionize the recently formed H atoms. Impressively also conversions at level $P_{a\gamma} \lesssim 10^{-9}$ would be enough to produce a seizable effect. Comparing this effect with the measurement of the optical depth in the Universe by the Planck experiment, we have shown that in principle it would be possible to obtain strong bounds on the ALP-photon coupling

$$g_{a\gamma}B \lesssim 6 \times 10^{-18} \text{ GeV}^{-1} \text{ nG} , \quad (5.1)$$

assuming that ALPs compose all the extra-radiation compatible with the 1σ bound of Planck ($\Delta N_{\text{eff}} = 0.38$). Intriguingly, if the primordial magnetic field would have a value close to

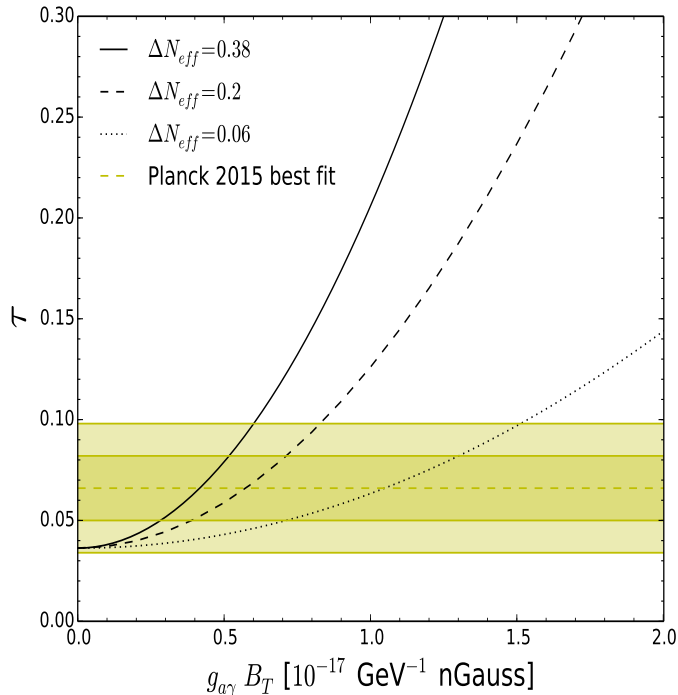


Figure 6. Optical depth τ in presence of ALP for $\Delta N_{\text{eff}} = 0.38$ (continuous curve), $\Delta N_{\text{eff}} = 0.2$ (dashed curve) and $\Delta N_{\text{eff}} = 0.06$ (dotted curve) in function of $g_{a\gamma} B$. The horizontal bands represent the 1σ (dark) and 2σ (light) range for τ measured from Planck. (see the text for details)

the present limits ($\sim \text{nG}$), Eq. (5.1) sets a limit on $g_{a\gamma}$ close to inverse of the Planck scale. (At this scale it has shown in [41] that the graviton would take the role of an ALP with $g_{a\gamma} \sim M_{\text{pl}}^{-1}$).

We stress that without direct evidence for a primordial magnetic field, our bounds do not allow to constrain directly the coupling constant $g_{a\gamma}$. However, even if a primordial magnetic field would be measured with values much lower than the current upper bound, $B \sim \text{nG}$, Eq. (5.1) would strongly constrain the phenomenological consequences of the cosmic ALP background. Indeed, the X-ray excess would typically require a coupling $g_{a\gamma} \sim 10^{-13} \text{ GeV}^{-1}$ [35–37]. Conversely, if the ALP interpretation of X-ray excess would be confirmed, Eq. (5.1) would provide the strongest constraint of the primordial magnetic field at the recombination epoch. Therefore, it is nice to realize that our cosmological limits from reionization could have relevant consequences for signatures of cosmic ALPs in X-ray sources. This confirms once more the nice synergy between astrophysics and cosmology to search axion-like particles.

Acknowledgments

We acknowledge Andrea Ferrara, Tetsutaro Higaki, Kazunori Nakayama, Fuminobu Takahashi and David J. E. Marsh for useful comments on the manuscript. The work of A.M. and D.M. is supported by the Italian Ministero dell’Istruzione, Università e Ricerca (MIUR) and Istituto Nazionale di Fisica Nucleare (INFN) through the “Theoretical Astroparticle Physics”

project. The work of M.L. is supported by the European Research Council under ERC Grant “NuMass” (FP7- IDEAS-ERC ERC-CG 617143).

Appendix: Approximate expression for ALP-photon conversion probability

In this Appendix we present the derivation of an approximate expression for the ALP-photon conversion probabilities suitable for our purposes. We realize that for the input parameters chosen in Eq. (3.5) it results

$$\Delta_{a\gamma} \ll \Delta_{pl}. \quad (5.2)$$

This hierarchy is valid independently of the redshift since $\Delta_{a\gamma}$ and Δ_{pl} both scale as $(1+z)^2$ (see Fig. 2). Including the absorption term Γ and neglecting Δ_{QED} , we rewrite the Hamiltonian [Eq. (3.3)], up to an overall term proportional to $\Delta_a \mathbb{I}_{3 \times 3}$ as

$$\mathcal{M}_p = \begin{pmatrix} k - i\frac{\Gamma}{2} & 0 & \Delta_{a\gamma} \cos \psi_p \\ 0 & k - i\frac{\Gamma}{2} & \Delta_{a\gamma} \sin \psi_p \\ \Delta_{a\gamma} \cos \psi_p & \Delta_{a\gamma} \sin \psi_p & 0 \end{pmatrix}, \quad (5.3)$$

where we have defined $k \equiv \Delta_{\text{CMB}} + \Delta_{pl} - \Delta_a$. Introducing this change of variables

$$A_{1,2} = \hat{A}_{1,2} \exp \left\{ -i \int_0^{x_3} ds \left(k(s) - i\frac{\Gamma(s)}{2} \right) \right\} \equiv \hat{A}_{1,2} e^{-\alpha(x_3)}, \quad (5.4)$$

the evolution equations acquire the form

$$i \frac{\partial}{\partial x_3} \begin{pmatrix} \hat{A}_1 \\ \hat{A}_2 \\ a \end{pmatrix} = \begin{pmatrix} 0 & 0 & \Delta_{a\gamma} \cos \psi_p e^\alpha \\ 0 & 0 & \Delta_{a\gamma} \sin \psi_p e^\alpha \\ \Delta_{a\gamma} \cos \psi_p e^{-\alpha} & \Delta_{a\gamma} \sin \psi_p e^{-\alpha} & 0 \end{pmatrix} \begin{pmatrix} \hat{A}_1 \\ \hat{A}_2 \\ a \end{pmatrix}. \quad (5.5)$$

Since $\Delta_{a\gamma} \ll \Delta_{pl}$ and $\Delta_{a\gamma} x_3 \ll 1$ we can expand at the first order the solution of the system (5.5)

$$\begin{aligned} \hat{A}_1(x_3) &= -i \int_0^{x_3} d\eta \Delta_{a\gamma} \cos \psi_p(\eta) e^{\alpha(\eta)} a(0) \\ \hat{A}_2(x_3) &= -i \int_0^{x_3} d\eta \Delta_{a\gamma} \sin \psi_p(\eta) e^{\alpha(\eta)} a(0). \end{aligned} \quad (5.6)$$

We assume that initially the beams is composed by only ALPs, so that $a(0) = 1$, while $\hat{A}_{1,2}(0) = 0$. Then the probability that an ALP is converted into a photon is given by

$$P_{a \rightarrow \gamma}(x_3) = |A_1(x_3)|^2 + |A_2(x_3)|^2 = \left(\left| \hat{A}_1(x_3) \right|^2 + \left| \hat{A}_2(x_3) \right|^2 \right) e^{-\int_0^{x_3} ds \Gamma(s)}, \quad (5.7)$$

where from Eq. (5.6)

$$\hat{A}_1(x_3) = -i \frac{g_{a\gamma}}{2} \int_0^{x_3} d\eta B_1(\eta) e^{\alpha(\eta)}, \quad (5.8)$$

with $B_1(\eta) = B_T(\eta) \cos \psi_p(\eta)$. Assuming a cell-like structure for the B -field, the previous integral can be written as

$$\hat{A}_1(x_3) = -i \frac{g_{a\gamma}}{2} \sum_{p=1}^n B_{1,p} \int_{x_{3,p}}^{x_{3,p+1}} d\eta e^{\alpha(\eta)}, \quad (5.9)$$

where $[x_{3,p}, x_{3,p+1}]$ is the interval of p -th and $B_{1,p}$ is the value of the magnetic field therein. Then, averaging over all the possible magnetic field configuration we get

$$\left\langle \left| \hat{A}_1(x_3) \right|^2 \right\rangle = \frac{g_{a\gamma}^2}{8} \sum_{p=1}^n (B_T^2)_p \int_{x_{3,p}}^{x_{3,p+1}} d\eta_1 d\eta_2 e^{i \int_{\eta_1}^{\eta_2} ds k(s)} e^{\int_0^{x_{3,p}} ds \Gamma(s)}, \quad (5.10)$$

where we used that $\alpha \equiv k - i\Gamma/2$ and assumed $\Gamma(s)$ constant in each cell. Assuming also $k(s)$ constant in each cell, we get

$$\left\langle \left| \hat{A}_1(x_3) \right|^2 \right\rangle = \frac{g_{a\gamma}^2}{8} \sum_{p=1}^n (B_T^2)_p \int_{x_{3,p}}^{x_{3,p+1}} d\eta_1 d\eta_2 e^{ik(\eta_1)(\eta_2 - \eta_1)} e^{\int_0^{x_{3,p}} ds \Gamma(s)}. \quad (5.11)$$

An analogous expression occurs for $\left\langle \left| \hat{A}_2(x_3) \right|^2 \right\rangle$. Then the conversion probability into photons assumes the form

$$P_{a \rightarrow \gamma}(x_3) = \frac{g_{a\gamma}^2}{4} \sum_{p=1}^n (B_T^2)_p \left| \int_{x_{3,p}}^{x_{3,p+1}} d\eta e^{-ik(\eta)\eta} \right|^2 e^{-\int_{x_{3,p}}^{x_3} ds \Gamma(s)}. \quad (5.12)$$

Using the Fourier transform of the hat function, this equation can be written as

$$P_{a \rightarrow \gamma}(x_3) = \frac{g_{a\gamma}^2}{4} \sum_{p=1}^n (B_T^2)_p l_p^2 \text{sinc}^2 \left(\frac{k_p l_p}{2} \right) e^{-\int_{x_{3,p}}^{x_3} ds \Gamma(s)}, \quad (5.13)$$

where $\text{sinc}(x) \equiv \sin(x)/x$, $l_p = |x_{3,p+1} - x_{3,p}|$ is the size of each cell and $k_p \equiv k(x_{3,p})$. Finally, we can write a recursive expression for the conversion probability in the n -th magnetic domain

$$P_{a\gamma}^{(n+1)} = \left[P_{a\gamma}^{(n)} + (\Delta_{a\gamma}^{(n)} l_n)^2 \text{sinc}^2 \frac{k_n l_n}{2} \right] e^{-\Gamma_n l_n} \quad (5.14)$$

where the subscript n refer to the values of the different quantities at redshift z_n .

A brief remark is in order. A very similar expansion can be obtained in the case of a more realistic homogeneous and isotropic turbulent magnetic field, where the Fourier components are correlated as [14]

$$\langle \tilde{B}_i(\mathbf{k}) \tilde{B}_j(\mathbf{k}') \rangle = (2\pi)^6 M(|\mathbf{k}|) \cdot \left(\delta_{ij} - \frac{k_i k_j}{|\mathbf{k}|^2} \right) \delta^3(\mathbf{k} - \mathbf{k}'), \quad (5.15)$$

(where the tensor in bracket implements the condition $\nabla \cdot \mathbf{B} = 0$). At first order, after straightforward calculations we obtain

$$P_{a \rightarrow \gamma}(x_3) = \frac{g_{a\gamma}^2}{2} \int_0^{x_3} ds \tilde{\varepsilon}_\perp(k(s)) e^{-\int_s^{x_3} du \Gamma(u)}, \quad (5.16)$$

(we omit the proof), where $\tilde{\varepsilon}_\perp(k)$ is the Fourier transform of the correlation function $\mathcal{C}(y) = \langle B_1(x_3) B_1(x_3 + y) \rangle$ along the line-of-sight.

For a cell-like structure $\langle B_1(x_3) B_1(x_3 + y) \rangle = \langle B_{1,p}(x_3) B_{1,p}(x_3 + y) \rangle$ where p is any of the cells along the line-of-sight, while the correlation between adjacent cells is zero. Since

$B_{1,p}(x_3)$ is a hat function with width l we have $\mathcal{C}(y) = B_T^2 \cdot (1 - |y|/l)$ for $|y| \leq l$ and zero otherwise, whose Fourier transform is just

$$\tilde{\varepsilon}_\perp(k) = \frac{1}{2} B_T^2 l \operatorname{sinc}^2\left(\frac{kl}{2}\right). \quad (5.17)$$

In this case Eq. (5.16) returns Eq. (5.13). For a Kolmogorov-like power-law spectrum $M(|\mathbf{k}|) \sim |\mathbf{k}|^q$ with $k_L \leq |\mathbf{k}| \leq k_H$ the function $\tilde{\varepsilon}_\perp(k)$ has been calculated in [21] [Eqs. (A.9–16)]. We have explicitly checked that the results are similar to those obtained for a cell-like structure for several choices of the spectral index q and cut-off parameters $k_{H,L}$. This shows that the choice of the cell-like structure for the magnetic field is not crucial for our results.

References

- [1] C. Coriano and N. Irges, “Windows over a New Low Energy Axion,” *Phys. Lett. B* **651**, 298 (2007) doi:10.1016/j.physletb.2007.06.022 [hep-ph/0612140].
- [2] H. Baer, M. Haider, S. Kraml, S. Sekmen and H. Summy, “Cosmological consequences of Yukawa-unified SUSY with mixed axion/axino cold and warm dark matter,” *JCAP* **0902**, 002 (2009) doi:10.1088/1475-7516/2009/02/002 [arXiv:0812.2693 [hep-ph]].
- [3] N. Turok, “Almost Goldstone bosons from extra dimensional gauge theories,” *Phys. Rev. Lett.* **76**, 1015 (1996) doi:10.1103/PhysRevLett.76.1015 [hep-ph/9511238].
- [4] P. Svrcek and E. Witten, “Axions In String Theory,” *JHEP* **0606**, 051 (2006) doi:10.1088/1126-6708/2006/06/051 [hep-th/0605206].
- [5] A. Arvanitaki, S. Dimopoulos, S. Dubovsky, N. Kaloper and J. March-Russell, “String Axiverse,” *Phys. Rev. D* **81**, 123530 (2010) doi:10.1103/PhysRevD.81.123530 [arXiv:0905.4720 [hep-th]].
- [6] M. Cicoli, M. Goodsell and A. Ringwald, “The type IIB string axiverse and its low-energy phenomenology,” *JHEP* **1210**, 146 (2012) doi:10.1007/JHEP10(2012)146 [arXiv:1206.0819 [hep-th]].
- [7] J. Jaeckel and A. Ringwald, “The Low-Energy Frontier of Particle Physics,” *Ann. Rev. Nucl. Part. Sci.* **60**, 405 (2010) doi:10.1146/annurev.nucl.012809.104433 [arXiv:1002.0329 [hep-ph]].
- [8] K. Ehret *et al.*, “New ALPS Results on Hidden-Sector Lightweights,” *Phys. Lett. B* **689**, 149 (2010) doi:10.1016/j.physletb.2010.04.066 [arXiv:1004.1313 [hep-ex]].
- [9] M. Arik *et al.* [CAST Collaboration], “New solar axion search using the CERN Axion Solar Telescope with ^4He filling,” *Phys. Rev. D* **92**, no. 2, 021101 (2015) doi:10.1103/PhysRevD.92.021101 [arXiv:1503.00610 [hep-ex]].
- [10] I. G. Irastorza *et al.*, “Towards a new generation axion helioscope,” *JCAP* **1106**, 013 (2011) doi:10.1088/1475-7516/2011/06/013 [arXiv:1103.5334 [hep-ex]].
- [11] S. J. Asztalos *et al.* [ADMX Collaboration], “A SQUID-based microwave cavity search for dark-matter axions,” *Phys. Rev. Lett.* **104**, 041301 (2010) doi:10.1103/PhysRevLett.104.041301 [arXiv:0910.5914 [astro-ph.CO]].
- [12] D. Horns, J. Jaeckel, A. Lindner, A. Lobanov, J. Redondo and A. Ringwald, “Searching for WISPy Cold Dark Matter with a Dish Antenna,” *JCAP* **1304**, 016 (2013) doi:10.1088/1475-7516/2013/04/016 [arXiv:1212.2970 [hep-ph]].
- [13] P. W. Graham, I. G. Irastorza, S. K. Lamoreaux, A. Lindner and K. A. van Bibber, “Experimental Searches for the Axion and Axion-Like Particles,” *Ann. Rev. Nucl. Part. Sci.* **65**, 485 (2015) doi:10.1146/annurev-nucl-102014-022120 [arXiv:1602.00039 [hep-ex]].

- [14] A. Mirizzi, G. G. Raffelt and P. D. Serpico, “Signatures of axion-like particles in the spectra of TeV gamma-ray sources,” *Phys. Rev. D* **76**, 023001 (2007) doi:10.1103/PhysRevD.76.023001 [arXiv:0704.3044 [astro-ph]].
- [15] A. De Angelis, M. Roncadelli and O. Mansutti, “Evidence for a new light spin-zero boson from cosmological gamma-ray propagation?,” *Phys. Rev. D* **76**, 121301 (2007) doi:10.1103/PhysRevD.76.121301 [arXiv:0707.4312 [astro-ph]].
- [16] M. Simet, D. Hooper and P. D. Serpico, “The Milky Way as a Kiloparsec-Scale Axionscope,” *Phys. Rev. D* **77**, 063001 (2008) doi:10.1103/PhysRevD.77.063001 [arXiv:0712.2825 [astro-ph]].
- [17] A. Mirizzi and D. Montanino, “Stochastic conversions of TeV photons into axion-like particles in extragalactic magnetic fields,” *JCAP* **0912**, 004 (2009) doi:10.1088/1475-7516/2009/12/004 [arXiv:0911.0015 [astro-ph.HE]].
- [18] D. Horns, L. Maccione, M. Meyer, A. Mirizzi, D. Montanino and M. Roncadelli, “Hardening of TeV gamma spectrum of AGNs in galaxy clusters by conversions of photons into axion-like particles,” *Phys. Rev. D* **86**, 075024 (2012) doi:10.1103/PhysRevD.86.075024 [arXiv:1207.0776 [astro-ph.HE]].
- [19] D. Horns and M. Meyer, “Indications for a pair-production anomaly from the propagation of VHE gamma-rays,” *JCAP* **1202**, 033 (2012) doi:10.1088/1475-7516/2012/02/033 [arXiv:1201.4711 [astro-ph.CO]].
- [20] M. Meyer, D. Horns and M. Raue, “First lower limits on the photon-axion-like particle coupling from very high energy gamma-ray observations,” *Phys. Rev. D* **87**, no. 3, 035027 (2013) doi:10.1103/PhysRevD.87.035027 [arXiv:1302.1208 [astro-ph.HE]].
- [21] M. Meyer, D. Montanino and J. Conrad, “On detecting oscillations of gamma rays into axion-like particles in turbulent and coherent magnetic fields,” *JCAP* **1409** (2014) 003 doi:10.1088/1475-7516/2014/09/003 [arXiv:1406.5972 [astro-ph.HE]].
- [22] A. De Angelis, G. Galanti and M. Roncadelli, “Relevance of axion-like particles for very-high-energy astrophysics,” *Phys. Rev. D* **84**, 105030 (2011) [*Phys. Rev. D* **87**, no. 10, 109903 (2013)] doi:10.1103/PhysRevD.87.109903, 10.1103/PhysRevD.84.105030 [arXiv:1106.1132 [astro-ph.HE]].
- [23] A. Mirizzi, G. G. Raffelt and P. D. Serpico, “Photon-axion conversion as a mechanism for supernova dimming: Limits from CMB spectral distortion,” *Phys. Rev. D* **72**, 023501 (2005) doi:10.1103/PhysRevD.72.023501 [astro-ph/0506078].
- [24] A. Mirizzi, G. G. Raffelt and P. D. Serpico, “Photon-axion conversion in intergalactic magnetic fields and cosmological consequences,” *Lect. Notes Phys.* **741**, 115 (2008) doi:10.1007/978-3-540-73518-2-7 [astro-ph/0607415].
- [25] A. Mirizzi, J. Redondo and G. Sigl, “Constraining resonant photon-axion conversions in the Early Universe,” *JCAP* **0908**, 001 (2009) doi:10.1088/1475-7516/2009/08/001 [arXiv:0905.4865 [hep-ph]].
- [26] D. J. E. Marsh, “Axion Cosmology,” arXiv:1510.07633 [astro-ph.CO].
- [27] M. Schlegeler and G. Sigl, “Constraining ALP-photon coupling using galaxy clusters,” *JCAP* **1601**, no. 01, 038 (2016) doi:10.1088/1475-7516/2016/01/038 [arXiv:1507.02855 [hep-ph]].
- [28] G. Mangano, G. Miele, S. Pastor, T. Pinto, O. Pisanti and P. D. Serpico, “Relic neutrino decoupling including flavor oscillations,” *Nucl. Phys. B* **729**, 221 (2005) doi:10.1016/j.nuclphysb.2005.09.041 [hep-ph/0506164].
- [29] P. A. R. Ade *et al.* [Planck Collaboration], “Planck 2015 results. XIII. Cosmological parameters,” arXiv:1502.01589 [astro-ph.CO].

- [30] S. Riemer-Sorensen, D. Parkinson and T. M. Davis, “What is half a neutrino? Reviewing cosmological constraints on neutrinos and dark radiation,” *Publ. Astron. Soc. Austral.* **30**, e029 (2013) doi:10.1017/pas.2013.005 [arXiv:1301.7102 [astro-ph.CO]].
- [31] M. Cicoli, J. P. Conlon and F. Quevedo, “Dark radiation in LARGE volume models,” *Phys. Rev. D* **87**, no. 4, 043520 (2013) doi:10.1103/PhysRevD.87.043520 [arXiv:1208.3562 [hep-ph]].
- [32] T. Higaki and F. Takahashi, “Dark Radiation and Dark Matter in Large Volume Compactifications,” *JHEP* **1211**, 125 (2012) doi:10.1007/JHEP11(2012)125 [arXiv:1208.3563 [hep-ph]].
- [33] T. Higaki, K. Nakayama and F. Takahashi, “Moduli-Induced Axion Problem,” *JHEP* **1307**, 005 (2013) doi:10.1007/JHEP07(2013)005 [arXiv:1304.7987 [hep-ph]].
- [34] J. P. Conlon and M. C. D. Marsh, “The Cosmophenomenology of Axionic Dark Radiation,” *JHEP* **1310**, 214 (2013) doi:10.1007/JHEP10(2013)214 [arXiv:1304.1804 [hep-ph]].
- [35] J. P. Conlon and M. C. D. Marsh, “Excess Astrophysical Photons from a 0.1?1 keV Cosmic Axion Background,” *Phys. Rev. Lett.* **111**, no. 15, 151301 (2013) doi:10.1103/PhysRevLett.111.151301 [arXiv:1305.3603 [astro-ph.CO]].
- [36] S. Angus, J. P. Conlon, M. C. D. Marsh, A. J. Powell and L. T. Witkowski, “Soft X-ray Excess in the Coma Cluster from a Cosmic Axion Background,” *JCAP* **1409**, no. 09, 026 (2014) doi:10.1088/1475-7516/2014/09/026 [arXiv:1312.3947 [astro-ph.HE]].
- [37] A. J. Powell, “A Cosmic ALP Background and the Cluster Soft X-ray Excess in A665, A2199 and A2255,” *JCAP* **1509**, no. 09, 017 (2015) doi:10.1088/1475-7516/2015/09/017 [arXiv:1411.4172 [astro-ph.CO]].
- [38] T. Higaki, K. Nakayama and F. Takahashi, “Cosmological constraints on axionic dark radiation from axion-photon conversion in the early Universe,” *JCAP* **1309**, 030 (2013) doi:10.1088/1475-7516/2013/09/030 [arXiv:1306.6518 [hep-ph]].
- [39] M. Mapelli, A. Ferrara and E. Pierpaoli, “Impact of dark matter decays and annihilations on reionization”, *Mon. Not. Roy. Astron. Soc.* **369**, 1719-1724 (2006) doi:10.1111/j.1365-2966.2006.10408.x [arXiv:astro-ph/0603237].
- [40] T. Basse, O. E. Bjaelde, J. Hamann, S. Hannestad and Y. Y. Y. Wong, “Dark energy properties from large future galaxy surveys,” *JCAP* **1405**, 021 (2014) doi:10.1088/1475-7516/2014/05/021 [arXiv:1304.2321 [astro-ph.CO]].
- [41] G. Raffelt and L. Stodolsky, “Mixing of the Photon with Low Mass Particles,” *Phys. Rev. D* **37**, 1237 (1988). doi:10.1103/PhysRevD.37.1237
- [42] P. Sikivie, “Experimental Tests of the Invisible Axion,” *Phys. Rev. Lett.* **51**, 1415 (1983) [*Phys. Rev. Lett.* **52**, 695 (1984)]. doi:10.1103/PhysRevLett.51.1415
- [43] A. A. Anselm, “Experimental Test for Axion γ - γ Photon Oscillations in a Homogeneous Constant Magnetic Field,” *Phys. Rev. D* **37**, 2001 (1988). doi:10.1103/PhysRevD.37.2001
- [44] A. Dobrynina, A. Kartavtsev and G. Raffelt, “Photon-photon dispersion of TeV gamma rays and its role for photon-ALP conversion,” *Phys. Rev. D* **91**, 083003 (2015) doi:10.1103/PhysRevD.91.083003 [arXiv:1412.4777 [astro-ph.HE]].
- [45] A. Ayala, I. Domnguez, M. Giannotti, A. Mirizzi and O. Straniero, “Revisiting the bound on axion-photon coupling from Globular Clusters,” *Phys. Rev. Lett.* **113**, no. 19, 191302 (2014) doi:10.1103/PhysRevLett.113.191302 [arXiv:1406.6053 [astro-ph.SR]].
- [46] A. Payez, C. Evoli, T. Fischer, M. Giannotti, A. Mirizzi and A. Ringwald, “Revisiting the SN1987A gamma-ray limit on ultralight axion-like particles,” *JCAP* **1502**, no. 02, 006 (2015) doi:10.1088/1475-7516/2015/02/006 [arXiv:1410.3747 [astro-ph.HE]].

- [47] R. Durrer and A. Neronov, “Cosmological Magnetic Fields: Their Generation, Evolution and Observation”, *Astron. Astrophys. Rev.* **21**, 62 (2013) doi:10.1007/s00159-013-0062-7 [arXiv:1303.7121 [astro-ph.CO]].
- [48] P. A. R. Ade *et al.* [Planck Collaboration], “Planck 2015 results. XIX. Constraints on primordial magnetic fields,” arXiv:1502.01594 [astro-ph.CO].
- [49] N. Bassan, A. Mirizzi and M. Roncadelli, “Axion-like particle effects on the polarization of cosmic high-energy gamma sources,” *JCAP* **1005**, 010 (2010) doi:10.1088/1475-7516/2010/05/010 [arXiv:1001.5267 [astro-ph.HE]].
- [50] M. Christensson and M. Fairbairn, “Photon-axion mixing in an inhomogeneous universe,” *Phys. Lett. B* **565**, 10 (2003) doi:10.1016/S0370-2693(03)00641-5 [astro-ph/0207525].
- [51] X. Fan and others, “A survey of $z > 5.7$ quasars in the sloan digital sky survey. 4. discovery of seven additional quasars,” *Astron. J.* **131**, 1203-1209 (2006) doi:10.1086/500296 [arXiv:astro-ph/0512080].
- [52] A. Ferrara and S. Pandolfi, “Reionization of the Intergalactic Medium,” *Proc. Int. Sch. Phys. Fermi* **186**, 1-57 (2014) doi:10.3254/978-1-61499-476-3-1 [arXiv:1409.4946 [astro-ph.CO]].
- [53] H. Jensen *et al.*, “Probing reionization with LOFAR using 21-cm redshift space distortions”, *Mon. Not. Roy. Astron. Soc.* **435**, 460 (2013) doi:10.1093/mnras/stt1341 [arXiv:1303.5627 [astro-ph.CO]].
- [54] S. Seager, D. D. Sasselov and D. Scott, “A New Calculation of the Recombination Epoch,” *ApJL* **523**, L1-L5 (1999) doi:10.1086/312250 [arXiv:astro-ph/9909275]
- [55] D. A. Verner, G. J. Ferland, K. T. Korista and D. G. Yakovlev, “Atomic data for astrophysics. 2. New analytic FITS for photoionization cross-sections of atoms and ions,” *Astrophys. J.* **465**, 487 (1996) doi:10.1086/177435 [astro-ph/9601009].
- [56] K. A. Olive *et al.* [Particle Data Group Collaboration], “Review of Particle Physics,” *Chin. Phys. C* **38**, 090001 (2014). doi:10.1088/1674-1137/38/9/090001
- [57] C. Evoli, M. Valdes, A. Ferrara and N. Yoshida, “Energy deposition by weakly interacting massive particles: a comprehensive study,” *Mon. Not. Roy. Astron. Soc.* **422**, 420 (2012). doi:10.1111/j.1365-2966.2012.20624.x
- [58] D. Syphers *et al.*, “He II $\text{Ly}\beta$ Gunn-Peterson Absorption: New HST Observations, and Theoretical Expectations”, *Astrophys. J.* **742**, 99 (2011) doi:10.1088/0004-637X/742/2/99 [arXiv:1108.4727 [astro-ph.CO]].
- [59] M. Cirelli, F. Iocco and P. Panci, “Constraints on Dark Matter annihilations from reionization and heating of the intergalactic gas,” *JCAP* **0910** (2009) 009 doi:10.1088/1475-7516/2009/10/009 [arXiv:0907.0719 [astro-ph.CO]].
- [60] A. Mesinger, “Understanding the Epoch of Cosmic Reionization,” Springer International Publishing, Switzerland, (2016) doi:10.1007/978-3-319-21957-8